J Sol-Gel Sci Technol (2017) 83:53–63
DOI 10.1007/s10971-017-4377-0

ORIGINAL PAPER: NANO- AND MACROPOROUS MATERIALS (AEROGELS, XEROGELS, CRYOGELS, ETC.)

Facile synthesis of large-sized monolithic methyltrimethoxysilane-based silica aerogel via ambient pressure drying

Shan Yun[1] · Tan Guo[1] · Jiadong Zhang[1] · Lei He[1] · Yanxing Li[1] · Huaju Li[1] · Xiufang Zhu[1] · Yanfeng Gao[2]

Received: 5 December 2016 / Accepted: 27 March 2017 / Published online: 7 April 2017

Abstract In this study, large-sized monolithic methyltrimethoxysilane-based silica aerogels were prepared via a facile sol–gel route using ambient pressure drying. The structural, morphological, and hydrophobic properties of the aerogels were characterized by scanning electron microscopy, transmission electron microscopy, Brunauer–Emmett–Teller method, and contact angle. Thermal conductivity, thermal stability, and mechanical properties of the samples were also evaluated. The ambient pressure dried aerogels showed macro-pore structure and low density (as low as 75 kg m^{-3}). The Young's modulus of the aerogels was observed to increase from 0.043 to 1.102 MPa with an increase in the density of the aerogels from 75 to 141 kg m^{-3}. Simultaneously, the aerogels exhibited superhydrophobicity (>150°), low thermal conductivity (0.036 W m^{-1} K^{-1}), and good thermal stability in air atmosphere. Both the simple fabricating process and the superior performance of the monolithic silica aerogel make it as a promising candidate for energy-saving sector.

Graphical Abstract Large-sized monolithic methyltrimethoxysilane-based silica aerogel with superhydrophobicity was successfully prepared by a one-step sol–gel method via ambient pressure drying using methyltrimethoxysilane as precursor, distilled water as solvent, and ammonia as alkali catalyst.

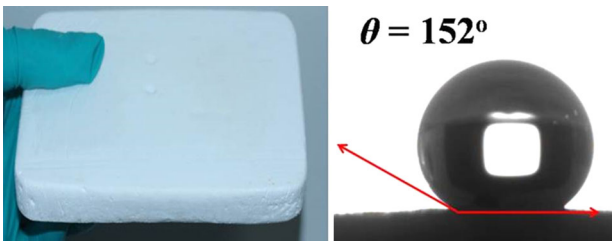

Keywords Silica aerogel · Methyltrimethoxysilane · Superhydrophobicity · Ambient pressure drying · Sol–gel

1 Introduction

Silica aerogel is a family of porous material with low density (3–500 kg m^{-3}) and high porosity (80–99.8%), and is a promising candidate for various applications ranging from Cherenkov radiation detector to super thermal insulator [1, 2]. Silica aerogel is generally synthesized by hydrolyzing and condensating of water glasses or silicon alkoxides to form gel, and followed by drying to remove a large amount of solvent. The fundamental requirement of drying is to retain the solid gel network to obtain aerogel [3]. The drying process is governed by the capillary pressure. However, the capillary pressure at the menisci of the solid–liquid–vapor interfaces inside the gel body usually results in serious shrinkage and cracking of the gel [4]. To avoid this issue, drying with a supercritical fluid (SCF) is generally employed. However, SCF drying requires high pressure and sometimes high temperature to transform the solvent in pores into its supercritical state, which usually

✉ Shan Yun
yunshan@hyit.edu.cn

[1] Jiangsu Provincial Engineering Laboratory for Advanced Materials of Salt Chemical Industry, Huaiyin Institute of Technology, Huai'an, Jiangsu 223003, China

[2] School of Materials Science and Engineering, Shanghai University, 99 Shangda, Shanghai 200444, China

must address issues such as cost, safety along with large-sized production [5, 6].

Compared with the expensive and time-consuming SCF drying process, the ambient pressure drying (APD) process proposed by Brinker's group [7, 8] is much cheaper and safer. Another important advantage of APD is that large-sized samples can be easily dried and prepared, especially for mass production [9–11]. To obtain high-porosity and crack-free monolithic aerogels by APD, two main strategies are usually used: increasing mechanical strength of the wet gel network by aging it in a silane precursor [12–15], and capping the surface silanol groups by alkyl groups to reduce the irreversible shrinkage [7, 16–21]. The porosities, densities, and specific surface areas of the silica aerogels obtained by APD are in the range of 93–94%, 120–150 kg m^{-3}, and >400 $m^2 g^{-1}$, respectively, which are comparable to those of samples prepared by SCF drying [21–23]. However, the surface treatment and solvent exchange steps are tedious and laborious for the reported APD procedures. In addition, during the surface modification procedure, violent reactions between the silylation agent and water in the pores of wet gel can result in insufficient surface modification of the silanol groups, which would increase the probabilities of crack generation and the subsequent failure of the monolith [24]. Hence, the large-scale production of monolithic silica aerogels synthesized via APD is still a challenge.

In order to avoid the surface modification step, the trifunctional organosilane compounds of the type $RSiX_3$ (where R is alkly, aryl or vinyl group, X is Cl or alkoxy group) were used as precursors to produce aerogels with good hydrophobicity [25–31]. Bhagat et al. [32] had developed a route to prepare methyltrimethoxysilane (MTMS)-based monolithic silica aerogels via APD. They used oxalic acid ($C_2H_2O_4$) and NH_4OH as acid and base catalyst, respectively, and controlled the methanol (MeOH)/MTMS ratio during the sol–gel process to yield aerogel with low bulk density of 62 kg m^{-3} and high surface area of 520 $m^2 g^{-1}$. In addition, the prepared aerogel was superhydrophobic with the contact angle as high as 152°. Xu et al. [33, 34] employed a similar method for producing MTMS-based monolithic aerogels at ambient pressure without the need for any solvent exchange and surface modification. They systematically investigated the effect of key processing parameters on the alcogel formation and macrostructures of the aerogel, and obtained monolithic aerogel with low bulk densities (65–76 kg m^{-3}) over a range of the precursor concentrations (MeOH/MTMS molar ratio from 27 to 36). Although impressive progress has been achieved in the preparation of monolithic aerogels by APD methods, the state of the art technics also suffer from the drawbacks like the using of toxic solvents and time-consuming processes.

In the present paper, we report a rapid, simple, and reproducible APD method for the large-scale production of large monolithic MTMS-based silica aerogels with low density (as low as 75 kg m^{-3}), superhydrophobicity (contact angle >150°), low thermal conductivity (as low as 0.036 W $m^{-1} K^{-1}$), and good thermal stability using MTMS as precursors, distilled water as solvent, and ammonia as alkali catalyst. The resultant precursor solution allows it for one-step sol–gel polymerization completed within 40 min by adjusting initial pH and concentration of the MTMS precursor. This facile process saves time, labor and space, and it is highly efficient for the mass production of monolithic silica aerogels.

2 Experimental section

2.1 Materials

MTMS (98%), cetyltrimethylammonium bromide (CTAB, 99.8%), and ammonium hydroxide ($NH_3 \cdot H_2O$, 28 wt.%) were purchased from Aladdin and used as received.

2.2 Synthesis of MTMS-based silica aerogels

The MTMS-based silica aerogels were fabricated by a one-step base catalyzed sol–gel process, followed by APD. Initially, the MTMS precursor was dissolved in aqueous CTAB solution (the concentration of CTAB was kept constant at 0.25 wt.%) under vigorous stirring for 30 min to obtain homogeneous silica solution at vary concentrations: 16 wt.%, 20 wt.%, 24 wt.%, 28 wt.% [35]. Second, ammonium hydroxide (the molar concentration of ammonium hydroxide was 14 mol L^{-1}) was added all at once to the solution under stirring, and then the solution was still kept stirring for several minutes before gelation. The pH value of the solution was adjusted from 7.5 to 10.0 in order to study the cracking and shrinking behaviors of the gels during APD and the physical properties of the resulting aerogels (the concentration of MTMS was fixed at 24 wt.%), and the total volume of the solution was 25.0, 24.0, 23.5, 23.0, 21.0, 20.5 mL as the pH value was 7.5, 8.0, 8.5, 9.0, 9.5, 10.0, respectively. The solutions were transferred into polystyrene containers, and the sealed containers were stored at room temperature (RT) for 3 h to complete the gelation and aging processes. The obtained gels were soaked in distilled water at 60 °C for 12 h, and the distilled water was exchanged three times every 12 h to remove the residual surfactant and chemicals. After that, the washed wet gels were dried at ambient pressure in a furnace in two subsequent steps as follows: at 80 °C for 24 h and, finally, at 120 °C for 12 h to obtain MTMS-based silica aerogels.

Table 1 Effects of pH values on the physical properties of MTMS-based aerogels, the concentration of MTMS was fixed at 24 wt.%

pH value	Gelation time (min)	Volume shrinkage (%)	Density (kg m^{-3})	Porosity (%)	A ($m^2\,g^{-1}$)	V_{pore} ($cm^3\,g^{-1}$)	D_{pore} (nm)	Remarks
7.5	No gel within 72 h	–	–	–	–	–	–	–
8.0	40	–	–	–	395.20	–	–	A few cracks
8.5	15	4.5	135	92.0	321.90	6.82	80	Surface crack
9.0	8	3.6	131	92.2	43.0	7.04	650	Monolith
9.5	6	2.5	125	92.6	33.68	7.41	880	Monolith
10.0	Precipitate	–	–	–	–	–	–	–

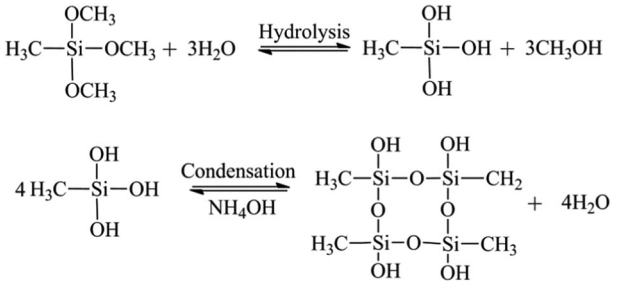

Fig. 1 The hydrolysis and condensation mechanism of the MTMS precursor in solution

2.3 Characterization methods

The bulk densities (ρ_b) of the obtained aerogels were calculated based on the ratio of mass to volume of gel. The skeletal density (ρ_s, ~1690 kg m^{-3}) was measured by helium pycnometry, and the porosities were calculated by Eq. (1).

$$\text{Porosity} = (1 - \rho_b/\rho_s) \times 100 \quad (1)$$

Specific surface areas (A) were calculated by the Brunauer–Emmett–Teller (BET) method using a Micromeritics Tristar 3000. Before measurement, the samples were degassed at 120 °C for 24 h until the mass attained a constant value. Due to mechanical deformation experienced by the aerogel samples in the capillary condensation range, pore volume and pore sizes obtained from BJH theory are unreliable. For this reason, pore volume V_{pore} and mean pore size D_{pore} were, respectively, calculated from Eqs. (2) and (3) [36].

$$V_{pore} = 1/\rho_b - 1/\rho_s \quad (2)$$

$$D_{pore} = 4V_{pore}/A \quad (3)$$

Microstructural studies of the aerogel samples were performed using field-emission scanning electron microscopy (FE-SEM, Hitachi, S-4800) and transmission electron microscopy (TEM, JEOL JEM-4000EX).

Compression tests were performed on cylindrical samples with a height-to-diameter ratio of 2:1 using an Instron 4505 test stand at a compression rate of 2 mm min^{-1}. The specimens were cut and polished to make sure that the top and bottom surfaces were smooth and parallel.

Contact angle (θ) measurements were performed using a contact angle meter (Kruss, DSA30) to quantify the degree of hydrophobicity of the aerogels. A 3 μL water droplet was placed at three different points on the surface of the aerogels, and the average value was taken as the contact angle (θ).

Fourier transform infrared spectroscopy (FTIR, Nicolet, Magna 560) was used to detect the chemical bonding of the aerogels.

The thermal conductivity of the aerogels was measured at RT with a HotDisk TPS2500 thermal constant analyzer, based on the transient hot plane method, using disk samples with a diameter of ~4 cm and a thickness of ~1 cm. The HotDisk probe was placed in the middle of two ends of the same samples and clamped tightly to prevent any bubbles from forming between the sample and the probe. The output power was 0.05 W, and the total transient time was 80 s. Each sample was tested three times to obtain an average value as the thermal conductivity.

Thermal stability of the aerogel was analyzed by means of thermal gravimetric analysis (TA Q600). The sample was heated from RT to 800 °C at a heating rate of 10 °C min^{-1} under air atmosphere.

X-ray powder diffraction (XRD) pattern was determined by a Philips X'Pert X-ray spectrometer using Cu K radiation with a tube voltage of 40 kV and a tube current of 35 mA.

3 Results and discussions

3.1 Rapid synthesis of crack-free monolithic MTMS-based silica aerogels

Conventionally, the MTMS-based silica aerogels were prepared by the two-step sol–gel process as described earlier [28, 32–34, 37]. However, it takes a long time (>24 h) to obtain wet gel and organic solvent is used. In the present study, we found that the gelation time of the silica sol (only distilled water as solvent) was greatly influenced by the pH

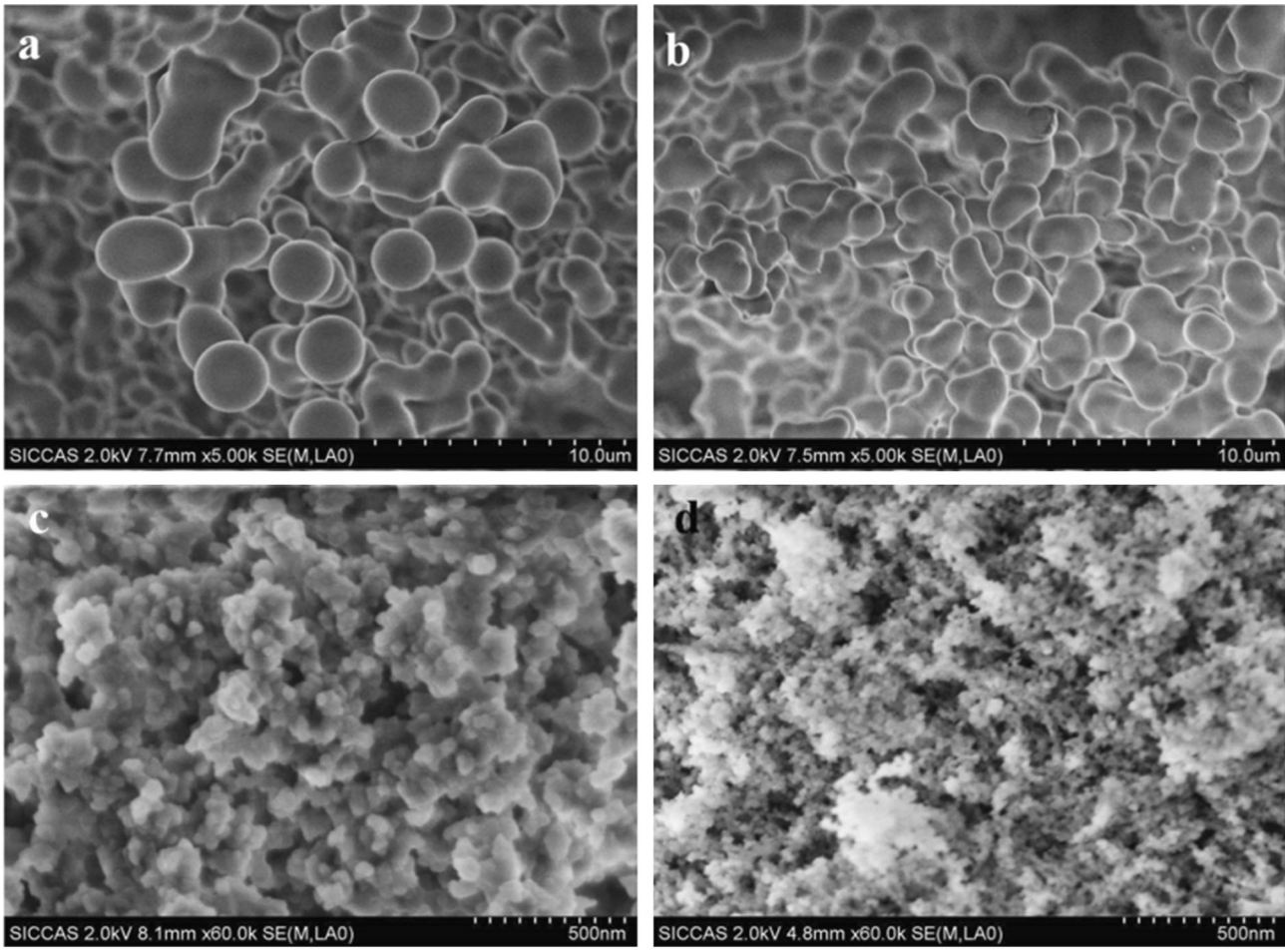

Fig. 2 FE-SEM images of MTMS-based silica aerogels prepared at different pH values, **a** 9.5, **b** 9.0, **c** 8.5, **d** 8.0

value of the solution (the concentration of MTMS was fixed at 24 wt.%). The gelation time sharply decreases as the increase of the pH value and it just needs several minutes to complete the gel formation at pH > 8.5 (see Table 1). It is noteworthy that when the pH value exceeds 10.0, precipitate is observed because of the rapid hydrolysis and condensation of MTMS precursor at a higher pH value. The reaction mechanism is shown in Fig. 1.

It is found that the physical properties of the silica aerogels are obviously affected by pH values. The volumetric shrinkage of the resulting aerogels decreases from 4.5 to 2.0% with increasing pH value from 8.5 to 9.5, leading to a decrease in density from 135 to 125 kg m^{-3} (see Table 1). In general, the aerogels obtained via APD show a shrinkage of 85–95% in volume after drying [38], due to the development of lateral compressive stress on the gel network to compensate for the loss of pore fluid and the surface silanol groups (Si–OH) of the adjacent silica clusters undergo condensation reactions, which result in an irreversible shrinkage of the gel network [39]. In our experiment, the shrinkage of the wet gel during APD can be easily controlled within 5%, which can be attributed to the fact that the hydrophobic methyl groups of the MTMS precursor reduce the chances of condensations of the surface silanol groups to prevent persistent shrinkage, and the repulsive interactions between hydrophobic moieties also promote the spring-back effect to reduce shrinkage [8]. The BET-specific surface area of the aerogels decreases from 395.2 to 33.68 $m^2 g^{-1}$, while the average pore size of the aerogels increases from 80 to 880 nm with an increase in pH value from 8.0 to 9.5 (see Table 1). The abrupt changes of these above results are due to the fact that a higher pH value can significantly accelerate the hydrolysis and the condensation of the MTMS precursors, result in forming larger silica particles and pore sizes as revealed by the FE-SEM images (see Fig. 2), and reducing the BET-specific surface areas remarkably.

Figure 3 shows the photographs of the MTMS-based silica aerogels prepared at different pH values of 8.0, 8.5, 9.0, and 9.5 (from right to left), respectively. It is clearly seen from Fig. 3 that the cracking probability during the APD of the gels decreases with an increase in the pH value

from 8.0 to 9.5. The gel cracks into small pieces for the lower pH value of 8.0 while the crack-free monolithic aerogels could be obtained for higher pH values of 9.0 and 9.5, which can be ascribed to the formation of larger pores at higher pH values (see Fig. 2 and Table 1). As a consequence, the capillary pressure (P_c) exerted on the gel network during the APD reduces considerably to avoid the collapse of the gel network.

As shown above, to get the crack-free aerogels with low shrinkage and density, the pH value should be kept at 9.5.

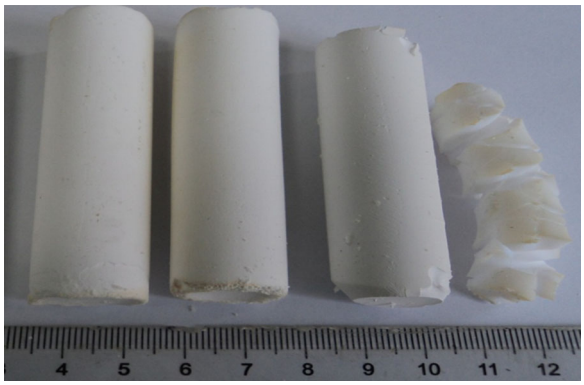

Fig. 3 The photo images of prepared MTMS-based silica aerogels at different pH values, from *left* to *right*: 9.5, 9.0, 8.5, 8.0

More significantly, MTMS-based silica aerogels could be easily manufactured with a large size using the proposed method. For example, a crack-free MTMS-based silica aerogel cuboid measuring ~240 cm^3 successfully prepared using a polystyrene mold (Fig. 4b). The properties of the crack-free monolithic aerogels (using cylindrical polystyrene containers as mold) prepared at the pH value of 9.5 were investigated below.

3.2 Microstructural and physical properties of monolithic MTMS-based aerogels

The physical properties of the monolithic MTMS-based aerogels can be tuned by changing the concentrations of the MTMS precursors (see Table 2). The volumetric shrinkage of the aerogel is lower than 5%, making it easy to control the density of MTMS-based aerogels. The density of aerogels increases from 75 to 141 kg m^{-3}, while the porosity decreases from 95.6 to 91.7%, as the precursor concentration varies from 16 to 28 wt.%. The densities and porosities of the aerogels developed in this study are comparable to those of silica aerogels (density: 100–300 kg m^{-3}, porosity: 60–95%) reported by Brinker [40]. In contrast to the earlier reports, it is observed that the gelation time increases with an increase in the precursor concentra-

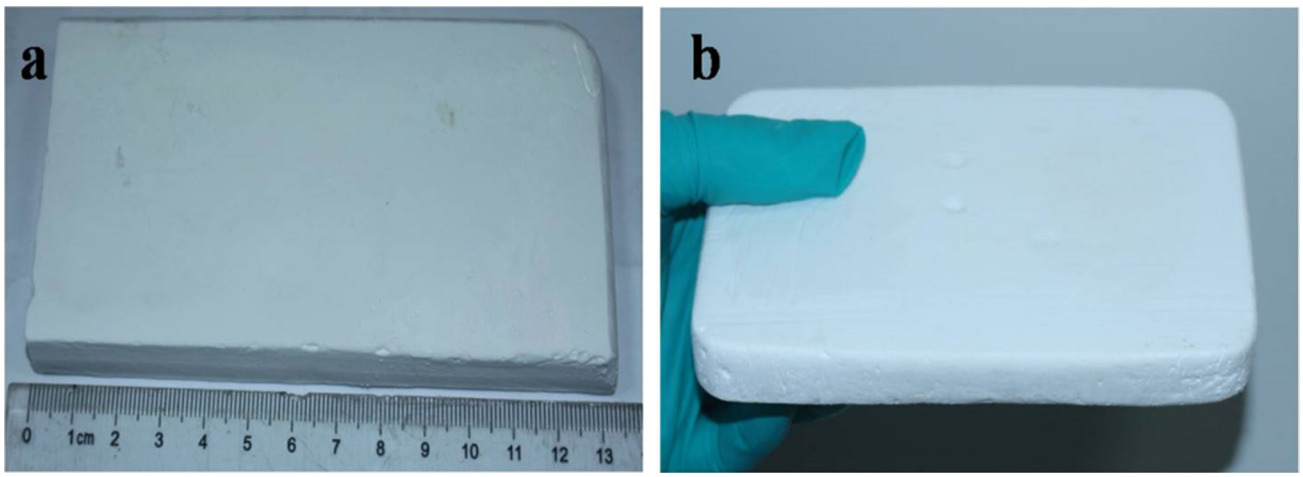

Fig. 4 Photo images of large-sized MTMS-based silica aerogels prepared at pH value of 9.5. **a** large-size aerogel cuboid (13.2 cm in length, 10.8 cm in width, and 1.1 cm in height) and **b** a 240 cm^3 aerogel cuboid (17 cm in length, 11.8 cm in width, and 1.2 cm in height)

Table 2 Physical properties of MTMS-based aerogels prepared at different concentration of MTMS, the pH value was fixed at 9.5

Concentration (wt.%)	Gelation time (min)	Volume shrinkage (%)	Density (kg m^{-3})	Porosity (%)	A (m^2 g^{-1})	V_{pore} (cm^3 g^{-1})	D_{pore} (nm)	Thermal conductivity (W m^{-1} K^{-1})
16	2.5	1.5	75	95.6	42.46	12.74	1200	0.038
20	4	2.0	105	93.8	37.60	8.93	950	0.036
24	6	2.5	125	92.6	33.68	7.41	880	0.041
28	10	3.2	141	91.7	30.58	6.50	850	0.044

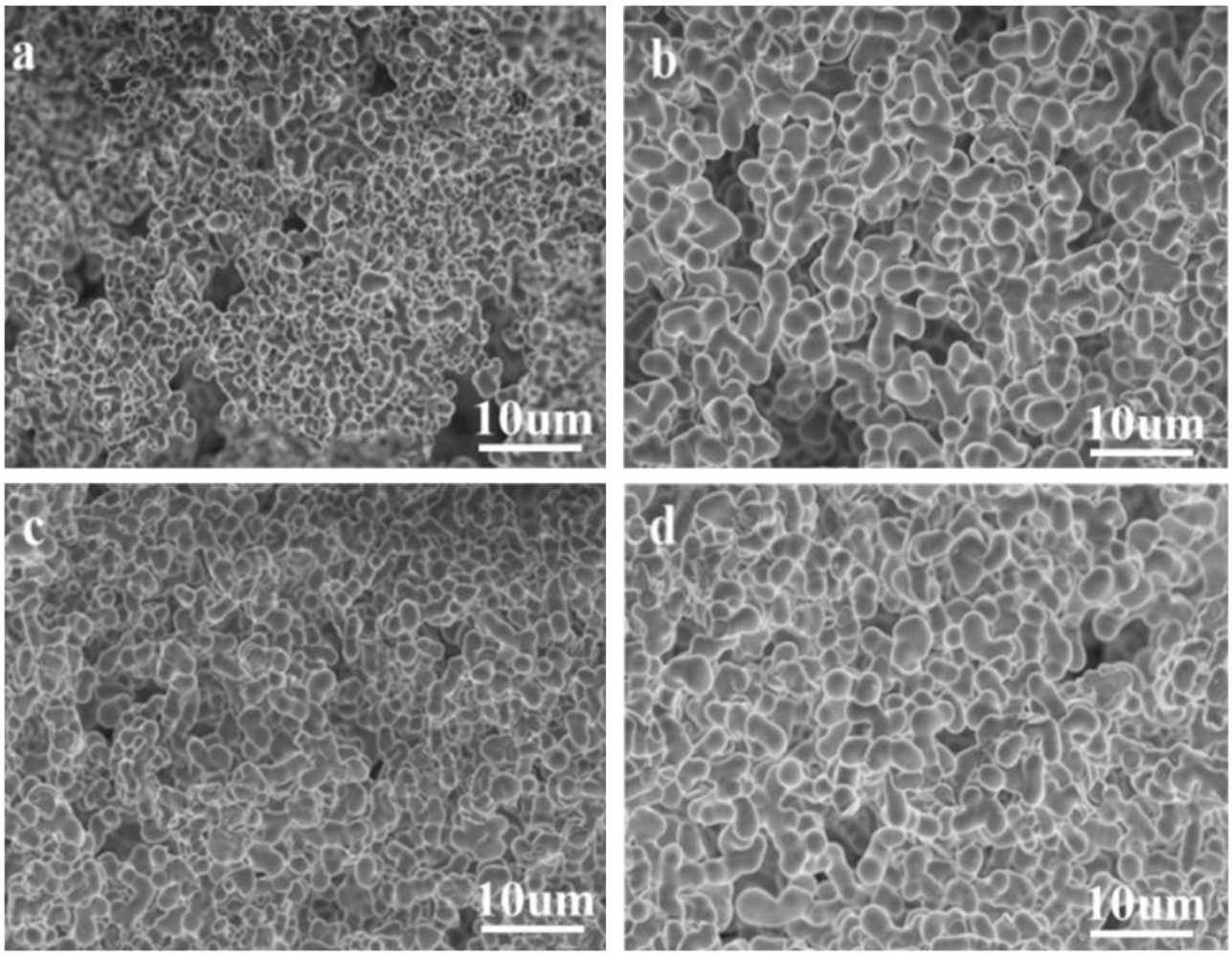

Fig. 5 FE-SEM images of MTMS-based silica aerogels prepared at different precursor concentration, **a** 16 wt.%, **b** 20 wt.%, **c** 24 wt.%, **d** 28 wt.%

tion [32]. This should be caused by the cyclic and cage-like closed species formed by MTMS, which would hinder the homogeneous gelling process, resulting in a longer gelation time as the concentration increased [37].

As shown in Fig. 5a–d, the aerogel frameworks are sparsely stacked by the smooth silica spheres, and larger pores are found at lower concentrations of the precursors. Meanwhile, the size of silica spheres increases from 500 to 1500 nm as the concentration of precursors increasing from 16 to 28 wt.% (Fig. 6a–d).

The specific surface areas of the aerogels are ranged from 42.46 to 30.58 $m^2 g^{-1}$ (Table 2), as calculated by the BET method, and the average pore sizes of the aerogels are ranged from 1200 to 850 nm as calculated from the Eq. (3). The specific surface areas seem to be lower than those of materials (500–1200 $m^2 g^{-1}$ for pure silica aerogel [41]). This can be attributed to: (1) the larger spherical particles making up the MTMS-based aerogels, which are one or two orders of magnitude larger than the particles in the pure silica aerogels; (2) the macropores formed in the MTMS-based aerogels.

The thermal conductivity of MTMS-based aerogels ranges from 0.036 to 0.044 $W m^{-1} K^{-1}$ (Table 2). These values are much lower than those of commercial silica gels (100–200 mesh, 0.098 $W m^{-1} K^{-1}$) and conventional inorganic thermal-insulation glass fibers (0.08 $W m^{-1} K^{-1}$). It is found that the MTMS-based aerogel with a density of 105 $kg m^{-3}$ shows the lowest thermal conductivity (see Table 2). As reported, thermal conductivity of aerogel materials is mainly composed of the gas-phase conduction and the solid-phase conduction [42–45]. Gaseous conductivity declines with the increased density because a higher solid content would result in a smaller pore size that suppresses gaseous thermal conductivity, while solid conductivity goes up with the increased density because the higher solid content brings about more effective solid thermal conduction. Since the thermal conductivity of the aerogel material is a trade-off between the gaseous conductivity and the solid conductivity, it is not hard to

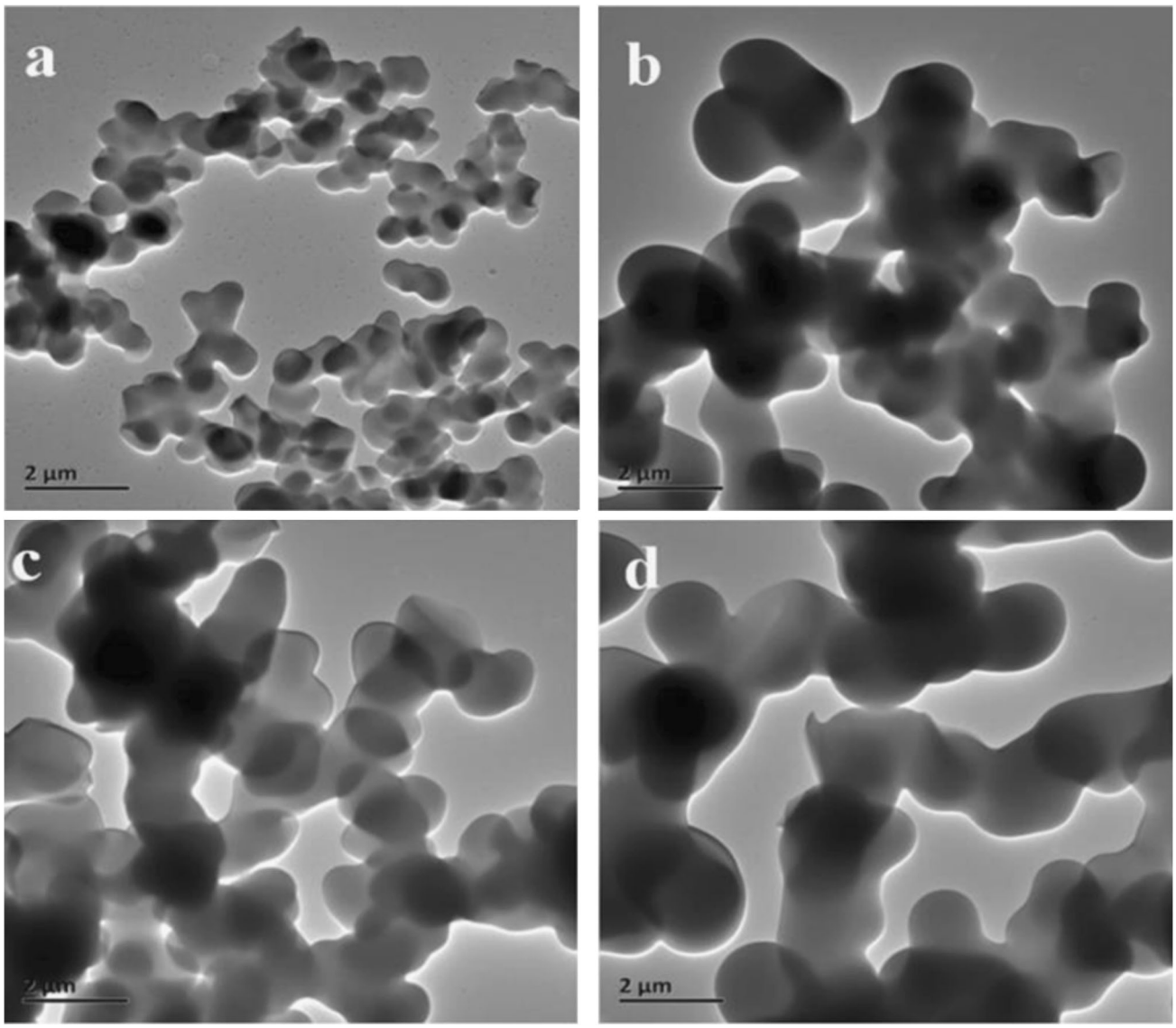

Fig. 6 TEM images of MTMS-based aerogels prepared at different precursor concentration, **a** 16 wt.%, **b** 20 wt.%, **c** 24 wt.%, **d** 28wt.%

understand why the lowest thermal conductivity is found at an intermediate density of 105 kg m^{-3}. Note that because the pore sizes (longer than the mean-free path of the gas molecules in air at ambient pressure (~70 nm)) are too large to confine gaseous thermal conductivity, it is reasonable that the MTMS-based aerogels presented in this work have higher thermal conductivities than those of typical silica aerogels (0.017–0.021 W m^{-1} K^{-1}) [2].

3.3 Mechanical properties of MTMS-based aerogels

Figure 7a shows the stress-strain curves from compression testing of the MTMS-based aerogels. It indicates that the mechanical strength of these aerogels increases with increasing density (increasing precursor concentration). The stress-strain curves of MTMS-based aerogels were similar to those of silica and other polymer-reinforced silica aerogels with a linear elastic region up to about 4–5% strain as well as exhibiting yield up to about 30–50% strain [6]. The slopes of the stress-strain curves in elastic regions are used to derive Young's modulus. The values of Young's modulus (E), the maximum compression strength (σ_{max}), and the corresponding strain (ε_{max}) obtained from these curves were summarized in Table 3. Young's modulus of these aerogels increases from 0.043 to 1.102 MPa as the density increasing from 75 to 141 kg m^{-3}, comparable to those of MTMS-based silica aerogel materials (Young's modulus: 0.014–0.034 MPa, density: 40–100 kg m^{-3}) reported by Rao et al. [28].

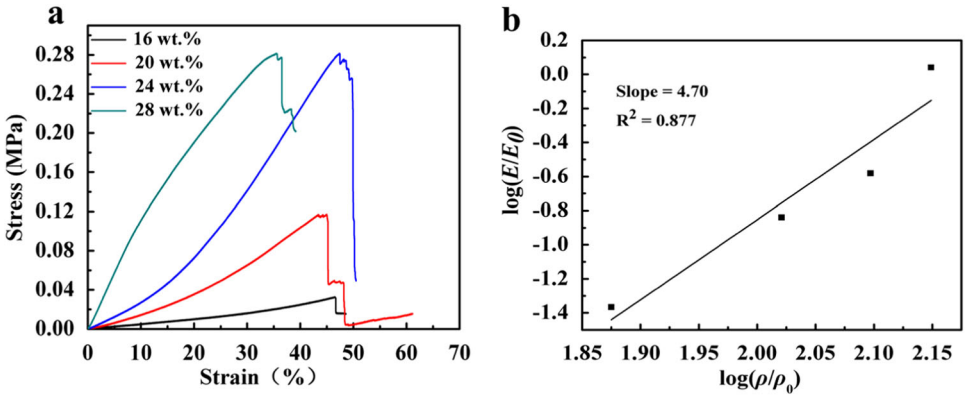

Fig. 7 **a** Stress-strain curves of the aerogels prepared with different precursor concentrations by compression test, and **b** Young's modulus is proportional to the logarithm of the density (slope = 4.70 and R^2 = 0.877)

Table 3 Properties of MTMS-based aerogels prepared with different precursor concentrations via APD

Sample	Density (kg m^{-3})	E (MPa)	σ_{max} (MPa)	ε_{max} (%)
16 wt.%	75	0.043	0.033	46.5
20 wt.%	105	0.145	0.114	43.4
24 wt.%	125	0.262	0.280	47.2
28 wt.%	141	1.102	0.281	35.5

The abrupt change of the mechanical properties for the sample of 24 wt.% ($E = 0.262$ MPa) compared with the sample of 28 wt.% ($E = 1.102$ MPa) was attributed to the fact that there is a power law relationship between Young's modulus (E) and density (ρ) of aerogels according to Eq. (4) [46]:

$$E = E_0(\rho/\rho_0)^m \quad (4)$$

where E is the Young's modulus (MPa), ρ is the density of aerogel (kg m^{-3}), m is the power exponent, and the index 0 denotes an arbitrary reference. Figure 7b shows that the logarithm of the Young's modulus is proportional to the logarithm of the density. The value of m is 4.70 as calculated from the slope, higher than the values ranging from 2.2 to 3.7 reported in the literature [47–49]. It is supposed that the neck width between adjacent particles increases with increasing the concentration of MTMS precursors (see Fig. 6), contributing to the improvement of Young's modulus.

3.4 Hydrophobic and thermal stability of the aerogels

The MTMS precursor (H_3C–Si–$(OCH_3)_3$) contains one non-hydrolyzable methyl group (–CH_3), and the in situ attachment of these hydrolytically stable –CH_3 groups to the siloxane backbone during the sol–gel polymerization leads to very low solid–liquid interfacial energy, which in turn results in a hydrophobic aerogel. The hydrophobicity was characterized by measuring the contact angle of the water droplet placed on the surface of aerogels. These water droplets have contact angles ranging from 152° to 162°, which is indicative of superhydrophobicity (see Fig. 8a). This superhydrophobicity is caused by the synergistic effect of two factors: one is the geometrically rough surface, derived from the porous structure; the other is the presence of methyl groups on the surface [37, 48], confirmed by FTIR spectra (Fig. 8b), where the peaks at 2960 and 1380 cm^{-1} can be assigned to the absorption of C–H of methyl groups, the peaks at 1200 cm^{-1} ascribed to the absorption of Si–C, the peaks at 1090 cm^{-1} being the asymmetrical stretch vibration of Si–O–Si, and the peaks at 799 cm^{-1}, 467 cm^{-1} attributed to the stretching and bending vibration absorption of Si–O [50].

The thermal stability of the MTMS-based silica aerogel (the density of aerogel is 105 kg m^{-3}) has been investigated by means of thermal gravimetric analysis. Figure 9 shows the TG curve of MTMS-based silica aerogel measured in the air atmosphere. The weight loss observed up to 175 °C is due to the evaporation of water molecules, and the dramatical decline in the weight observed over 450 °C is owing to the oxidation of the methyl groups. The structure, thermal conductivity, and hydrophobicity of the aerogel were also investigated after the following heat treatment process: the aerogel was heated from RT to 450 °C at a heating rate of 10 °C min^{-1}, then kept at 450 °C for 30 min in air. Figure 10 shows that the 3D networks and porous structures of the MTMS-based silica aerogel still remain after the heat treatment. Meanwhile, the contact angle slightly decreases to 149° and the thermal conductivity slightly increases to 0.038 W m^{-1} K^{-1}. Figure 11 shows the X-ray diffraction patterns of the unheated and heated aerogels. There are not any sharp peaks which indicates that the aerogel is still amorphous even after heating at 450 °C for 30 min in air. These results indicate that the texture of the aerogel has not been destroyed after the heat treatment at 450 °C. Above the temperature of 450 °C, the hydrophobicity of the aerogel becomes hydrophilicity in agreement with the reported results by Bhagat et al. [32].

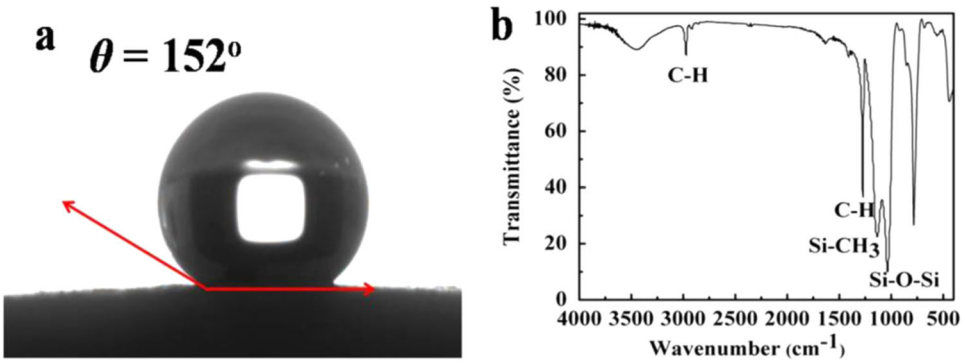

Fig. 8 **a** The contact angle of water on the surface of MTMS-based silica aerogel (density is 0.105) and **b** the FT-IR spectrum of MTMS-based silica aerogel

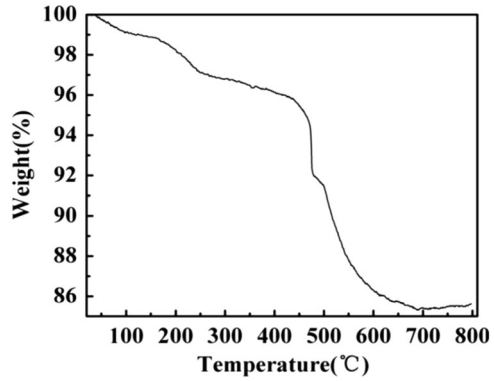

Fig. 9 TG curve of MTMS-based silica aerogel in an air atmosphere (heating rate was 10 °C min^{-1})

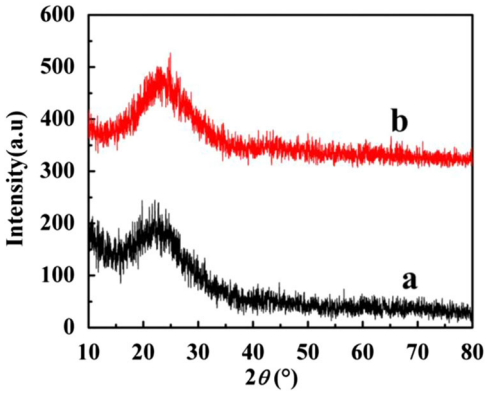

Fig. 11 XRD patterns of the MTMS-based aerogels **a** before heating and **b** after heating at 450 °C for 30 min

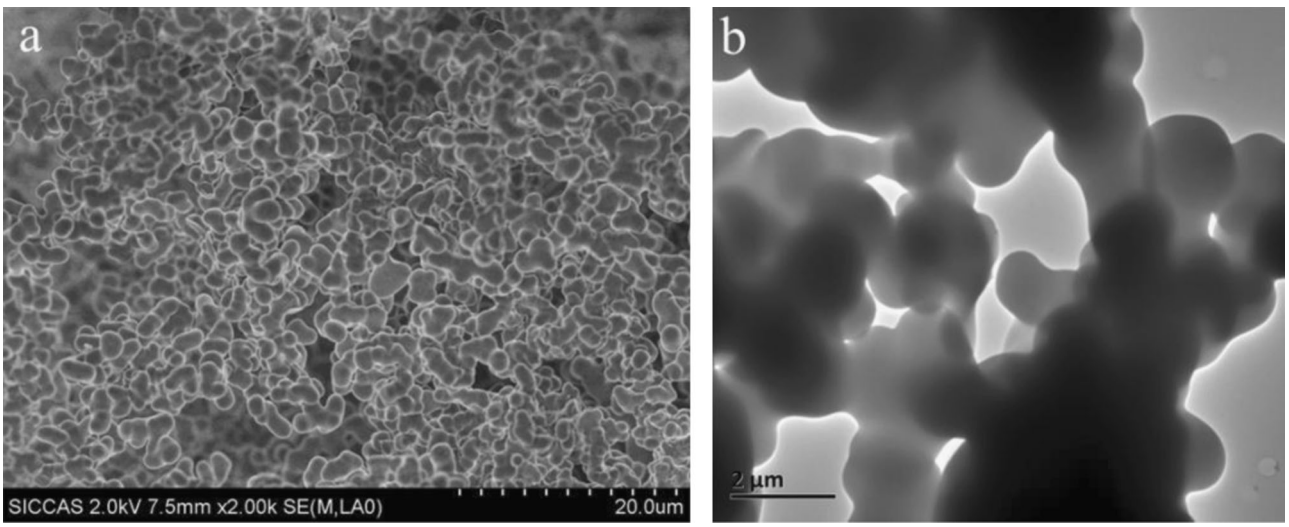

Fig. 10 The microstructures of MTMS-based silica aerogel after heat treatment at 450 °C for 30 min in air. **a** FE-SEM image and **b** TEM image

4 Conclusions

A more efficient, environmentally friendly approach was developed to get large-sized monolithic MTMS-based silica aerogels by adopting one-step sol–gel process for the pH value at 9.5 and distilled water as solvent. The MTMS-based silica aerogels achieved density as low as 75 kg m^{-3} and thermal conductivity as low as 0.036 W m^{-1} K^{-1}. The Young's modulus of these aerogels increased from 0.043 to 1.102 MPa as the density increasing from 75 to 141 kg m^{-3}.

The MTMS-based silica aerogels exhibited super-hydrophobicity and thermal stability up to a threshold temperature of 450 °C. These materials are useful in the long-term and large-scale application of thermal insulation for energy-saving practice.

Acknowledgements This study was financially supported by State Outstanding Young Scholars (contract No: 51325203), Opening Funding of Jiangsu Provincial Engineering Laboratory for Advanced Materials of Salt Chemical Industry (contract No: SF201506 and SF201507), and the Natural Science Foundation of Jiangsu Province (Grants No: BK20130420).

Conflict of interest The authors declare that they have no competing interests.

References

1. Schmidt M, Schwertfeger F (1998) Applications for silica aerogel products. J Non-Cryst Solids 225:364–368
2. Hüsing N, Schubert U (1998) Aerogels-airy materials: chemistry, structure, and properties. Angew Chem Int Ed 37:22–45
3. Kistler S (1932) Coherent expanded-aerogels. J Phys Chem 36:52–64
4. Scherer GW (1990) Theory of drying. J Am Ceram Soc 73:3–14
5. Leventis N, Lu H (2011) Polymer-crosslinked aerogels. In: Aegerter MA, Leventis N, Koebel MM (eds) Aerogels handbook, Springer, New York, p 251–285
6. Wei TY, Lu SY, Chang YC (2008) Transparent, hydrophobic composite aerogels with high mechanical strength and low high-temperature thermal conductivities. J Phys Chem B 112:11881–11886
7. Prakash SS, Brinker CJ, Hurd AJ (1995) Silica aerogel films at ambient pressure. J Non-Cryst Solids 190:264–275
8. Prakash SS, Hurd AJ, Rao SM, Brinker CJ (1995) Silica aerogel films prepared at ambient pressure by using surface derivatization to induce reversible drying shrinkage. Nature 374:439
9. Wang J, Zhang Y, Wei Y, Zhang X (2015) Fast and one-pot synthesis of silica aerogels via a quasi-solvent-exchange-free ambient pressure drying process. Micropor Mesopor Mater 218:192–198
10. Yun S, Luo H, Gao Y (2014) Ambient-pressure drying synthesis of large resorcinol-formaldehyde-reinforced silica aerogels with enhanced mechanical strength and superhydrophobicity. J Mater Chem A 2:14542–14549
11. Yun S, Luo H, Gao Y (2015) Low-density, hydrophobic, highly flexible ambient-pressure-dried monolithic bridged silsesquioxane aerogels. J Mater Chem A 3:3390–3398
12. Einarsrud MA, Nilsen E (1998) Strengthening of water glass and colloidal sol based silica gels by aging in TEOS. J Non-Cryst Solids 226:122–128
13. Rolison DR, Dunn B (2001) Electrically conductive oxide aerogels: new materials in electrochemistry. J Mater Chem 11:963–980
14. Haereid S, Dahle M, Lima S, Einarsrud MA (1995) Preparation and properties of monolithic silica xerogels from TEOS-based alcogels aged in silane solutions. J Non-Cryst Solids 186:96–103
15. Hæreid S, Nilsen E, Einarsrud MA (1996) Properties of silica gels aged in TEOS. J Non-Cryst Solids 204:228–234
16. Wei TY, Chang TF, Lu SY, Chang YC (2007) Preparation of monolithic silica aerogel of low thermal conductivity by ambient pressure drying. J Am Ceram Soc 90:2003–2007
17. Rao AP, Rao AV, Pajonk G (2007) Hydrophobic and physical properties of the ambient pressure dried silica aerogels with sodium silicate precursor using various surface modification agents. Appl Surf Sci 253:6032–6040
18. Sarawade PB, Shao GN, Quang DV, Kim HT (2013) Effect of various structure directing agents on the physicochemical properties of the silica aerogels prepared at an ambient pressure. Appl Surf Sci 287:84–90
19. He P, Gao XD, Li XM, Jiang ZW, Yang ZH, Wang CL, Gu ZY (2014) Highly transparent silica aerogel thick films with hierarchical porosity from water glass via ambient pressure drying. Mater Chem Phys 147:65–74
20. Shao Z, Luo F, Cheng X, Zhang Y (2013) Superhydrophobic sodium silicate based silica aerogel prepared by ambient pressure drying. Mater Chem Phys 141:570–575
21. Bangi UK, Jung IK, Park CS, Baek S, Park HH (2013) Optically transparent silica aerogels based on sodium silicate by a two step sol-gel process and ambient pressure drying. Solid State Sci 18:50–57
22. Schwertfeger F, Frank D, Schmidt M (1998) Hydrophobic waterglass based aerogels without solvent exchange or supercritical drying. J Non-Cryst Solids 225:24–29
23. Lee C, Kim G, Hyun S (2002) Synthesis of silica aerogels from waterglass via new modified ambient drying. J Mater Sci 37:2237–2241
24. Hwang SW, Kim TY, Hyun SH (2010) Effect of surface modification conditions on the synthesis of mesoporous crack-free silica aerogel monoliths from waterglass via ambient-drying. Micropor Mesopor Mater 130:295–302
25. Rao AV, Kulkarni MM, Pajonk GM, Amalnerkar DP, Seth T (2003) Synthesis and characterization of hydrophobic silica aerogels using trimethylethoxysilane as a co-precursor. J Sol-Gel Sci Techn 27:103–109
26. Rao AV, Kulkarni MM, Amalnerkar DP, Seth T (2003) Superhydrophobic silica aerogels based on methyltrimethoxysilane precursor. J Non-Cryst Solids 330:187–195
27. Ochoa M, Durães L, Beja A (2012) Portugal, study of the suitability of silica based xerogels synthesized using ethyltrimethoxysilane and/or methyltrimethoxysilane precursors for aerospace applications. J Sol-Gel Sci Techn 61:151–160
28. Rao AV, Bhagat SD, Hirashima H, Pajonk G (2006) Synthesis of flexible silica aerogels using methyltrimethoxysilane (MTMS) precursor. J Colloid Interf Sci 300:279–285
29. Nadargi DY, Rao AV (2009) Methyltriethoxysilane: new precursor for synthesizing silica aerogels. J Alloys Comp 467:397–404
30. Nadargi D, Latthe S, Rao AV (2009) Effect of post-treatment (gel aging) on the properties of methyltrimethoxysilane based silica aerogels prepared by two-step sol-gel process. J Sol-Gel Sci Techn 49:53–59
31. Aravind PR, Soraru GD (2011) High surface area methyltriethoxysilane-derived aerogels by ambient pressure drying. J Porous Mater 18:159–165
32. Bhagat SD, Oh CS, Kim YH, Ahn YS, Yeo JG (2007) Methyltrimethoxysilane based monolithic silica aerogels via ambient pressure drying. Micropor Mesopor Mater 100:350–355
33. Xu B, Cai JY, Xie Z, Wang L, Burgar I, Finn N, Cai Z, Wong L (2012) An improved method for preparing monolithic aerogels based on methyltrimethoxysilane at ambient pressure part II: microstructure and performance of the aerogels. Micropor Mesopor Mater 148:152–158
34. Xu B, Cai JY, Finn N, Cai Z (2012) An improved method for preparing monolithic aerogels based on methyltrimethoxysilane at ambient pressure part I: process development and macrostructures of the aerogels. Micropor Mesopor Mater 148:145–151

35. Yun S, Luo H, Gao Y (2014) Superhydrophobic silica aerogel microspheres from methyltrimethoxysilane: rapid synthesis via ambient pressure drying and excellent absorption properties. RSC Adv 4:4535–4542
36. Wong JC, Kaymak H, Tingaut P, Brunner S, Koebel MM (2015) Mechanical and thermal properties of nanofibrillated cellulose reinforced silica aerogel composites. Micropor Mesopor Mater 217:150–158
37. Kanamori K, Aizawa M, Nakanishi K, Hanada T (2007) New transparent methylsilsesquioxane aerogels and xerogels with improved mechanical properties. Adv Mater 19:1589–1593
38. Liu M, Gan L, Pang Y, Xu Z, Hao Z, Chen L (2008) Synthesis of titania-silica aerogel-like microspheres by a water-in-oil emulsion method via ambient pressure drying and their photocatalytic properties. Colloids Surf A Physicochem Eng Asp 317:490–495
39. Deshpande R, Hua DW, Smith DM, Brinker CJ (1992) Pore structure evolution in silica gel during aging/drying. III. Effects of surface tension. J Non-Cryst Solids 144:32–44
40. Brinker CJ, Deshpande R, Smith DM (1996) Preparation of high porosity xerogels by chemical surface modification. U.S. Patent No. 5,565,142.
41. Hrubesh L (1990) Aerogels: the world's lightest solids. Chem Ind 24:824–827.
42. Swimm K, Reichenauer G, Vidi S, Ebert HP (2009) Gas pressure dependence of the heat transport in porous solids with pores smaller than 10 μm. Int J Thermophys 30:1329–1342
43. Lu X, Schuster MA (1992) Thermal conductivity of monolithic organic aerogels. Science 255:971
44. Hayase G, Kanamori K, Abe K, Yano H, Maeno A, Kaji H, Nakanishi K (2014) Polymethylsilsesquioxane-cellulose nanofiber biocomposite aerogels with high thermal insulation, bendability, and superhydrophobicity. ACS Appl Mater Interf 6:9466–9471
45. Wang Z, Wang D, Qian Z, Guo J, Dong H, Zhao N, Xu J (2015) Robust superhydrophobic bridged silsesquioxane aerogels with tunable performances and their applications. ACS Appl Mater Interf 7:2016–2024
46. Groβ J, Fricke J (1995) Scaling of elastic properties in highly porous nanostructured aerogels. Nanostruct Mater 6:905–908
47. Parmenter KE, Milstein F (1998) Mechanical properties of silica aerogels. J Non-Cryst Solids 223:179–189
48. Girona MM, Roig A, Molins E, Martınez E, Esteve J (1999) Micromechanical properties of silica aerogels. Appl Phys Lett 75:653–655
49. Kucheyev S, Stadermann M, Shin S, Satcher J, Gammon S, Letts S, Van Buuren T, Hamza A (2012) Super-compressibility of ultralow-density nanoporous silica. Adv Mater 24:776–780
50. Yokogawa H, Yokoyama M (1995) Hydrophobic silica aerogels. J Non-Cryst Solids 18:23–29